

Review

# State of the Simulation of Mesoscale Winds in the Mediterranean and Opportunities for Improvements

Anika Obermann-Hellhund 

Institut für Atmosphäre und Umwelt, Goethe-Universität Frankfurt, 60629 Frankfurt, Germany; obermann@iau.uni-frankfurt.de

**Abstract:** The Mediterranean region is a densely populated and economically relevant area with complex orography including mountain ranges, islands, and straits. In combination with pressure gradients, this creates many mesoscale wind systems that cause, e.g., wind gusts and wildfire risk in the Mediterranean. This article reviews the recent state of the science of several mesoscale winds in the Mediterranean and associated processes. Previous work, including case studies on several time ranges and resolutions, as well as studies on these winds under future climate conditions, is discussed. Simulations with grid spacings of 25 to 50 km can reproduce winds driven by large-scale pressure patterns such as Mistral, Tramontane, and Etesians. However, these simulations struggle with the correct representation of winds channeled in straits and mountain gaps and around islands. Grid spacings of 1–3 km are certainly necessary to resolve these small-scale features. The smaller grid spacings are widely used in case studies, but not yet in simulations over large areas and long periods, which also could help to understand the interaction between small-scale phenomena in separate locations. Furthermore, by far not all Mediterranean straits, islands, and mountain gaps were studied in-depth and many interesting Mediterranean small-scale winds still need to be studied.

**Keywords:** Mediterranean area; mesoscale winds; regional climate models; straits; Mistral; Tramontane; Bora; Etesians; land breeze; sea breeze



**Citation:** Obermann-Hellhund, A. State of the Simulation of Mesoscale Winds in the Mediterranean and Opportunities for Improvements. *Atmosphere* **2022**, *13*, 1007. <https://doi.org/10.3390/atmos13071007>

Academic Editors: Xiao Dong, Jiangbo Jin and Hao Luo

Received: 2 June 2022  
Accepted: 20 June 2022  
Published: 22 June 2022

**Publisher's Note:** MDPI stays neutral with regard to jurisdictional claims in published maps and institutional affiliations.



**Copyright:** © 2022 by the author. Licensee MDPI, Basel, Switzerland. This article is an open access article distributed under the terms and conditions of the Creative Commons Attribution (CC BY) license (<https://creativecommons.org/licenses/by/4.0/>).

## 1. Introduction

The Mediterranean region is a densely populated area with complex orography that spans several climate zones. Its centerpiece is the Mediterranean Sea, a semi-enclosed sea connected to the Atlantic Ocean by the Strait of Gibraltar and to the Black Sea by the Dardanelles and the Bosphorus. Besides straits, it also features many islands with a wide range of sizes and complex coastlines. Several high mountain ranges—the Alps, Pyrenees, and the Taurus Mountains—with valleys of all sizes and shapes, surround the Mediterranean Sea (Figure 1). The diverse topography gives rise to many local and regional wind systems, which pose a threat to the local population through, e.g., wind gusts, increased wildfire risk, widespread distribution of aerosols, changes in precipitation, and intensified dust transport. The Mediterranean region is a hotspot of climate change [1,2]. Therefore, information on the wind systems and possible future changes is in a high need for risk, adaption, and mitigation studies.

Generally speaking, such information about past, present, and future climate can be obtained from natural climate archives and observation in combination with climate simulations. Global circulation models (GCMs) simulate the Earth's climate on a global scale with grid spacings of about 100 km. The resolution of these models is too coarse to sufficiently simulate local phenomena such as regional winds. This issue is addressed by regional climate models (RCMs), integrating the differential equations describing the atmosphere over a specific area with a higher resolution than the GCMs (downscaling). The coordinated regional climate downscaling experiment CORDEX [3,4] coordinates these efforts with a joint experimental framework. It covers the Mediterranean region

in two overlapping spatial domains: Med-CORDEX [5] and EURO-CORDEX [6]. At the borders of the simulation area, the results of a global simulation or another data set provide the lateral boundary conditions. Coupled RCMs add other spheres of the climate system to the atmosphere, e.g., the oceans, the hydrosphere, or the cryosphere. Due to limits in computing resources, studies usually investigate the challenges of simulating small-scale processes by simulating rather small areas and/or short periods, e.g., a few days, with very high resolution (i.e., in case studies as [7–10]). In the last years, increasing computing resources made high-resolution simulations over wider areas and longer periods possible.

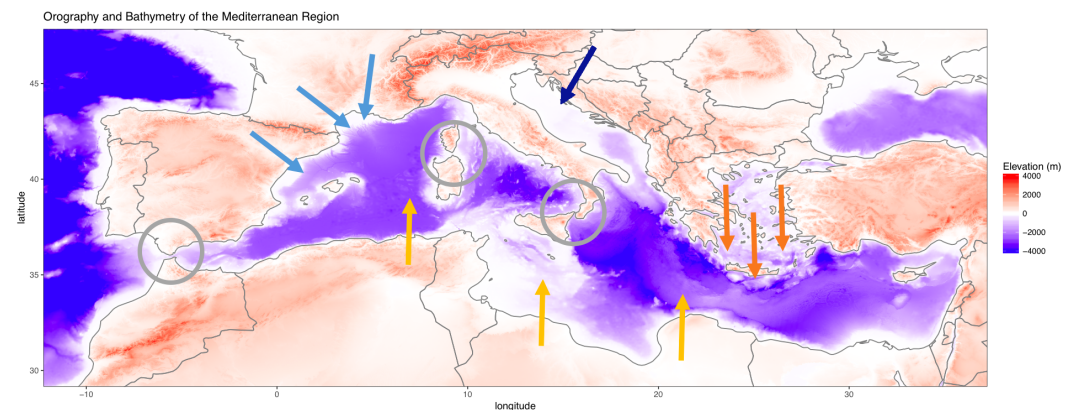


**Figure 1.** Mediterranean orography and bathymetry [11]. Arrows indicate mesoscale wind systems: winds channeled in valleys (light blue), Bora (dark blue), Etesians/Meltemi (orange), and southern dry winds (yellow). Circles indicate the Strait of Gibraltar, Strait of Bonifacio, and Strait of Messina (from west to east).

The investigated mesoscale winds are caused by pressure patterns on a wide range of spatial scales, often in conjunction with the local orography. This leads to complex wind fields and makes the classification of winds as regional winds, gap winds, and downslope windstorms, and several other types of wind difficult. Often a wind shows characteristics of several wind types. The categorization of winds is therefore necessarily often ambiguous. However, the winds in this review are sorted roughly by spatial scale, starting from larger-scale phenomena and moving to smaller scales.

This review gives an overview of recent modeling results for mesoscale winds in the Mediterranean region. It presents the characteristics of the winds and the processes that cause their distinctive wind patterns. The winds are categorized according to geographical location, wind speed and direction, temperature, as well as temporal and spatial scale. Furthermore, the existing work on mesoscale winds in the Mediterranean and the used modeling strategies are presented. This includes using different models with a wide range of grid spacings, both in case studies and climate simulations. The state of the art in simulating Mediterranean mesoscale winds is summarized and the most pressing issues are discussed. Emphasis is put on providing comprehensive insights on the necessary grid spacing for sufficient simulation of different processes versus deeper insight to be gained by coupled simulations. Thus, this review aims to answer the following questions:

- For which winds do high-resolution simulations exist and do they provide additional insights?
- Which Mediterranean wind systems have already been studied in detail, and which wind systems have only little data available and appear promising for further study?
- Which grid spacing is needed to resolve phenomena such as gap winds, sea breeze, and wave breaking?
- Which model improvements—besides higher resolution—are needed?

The following sections introduce the Mediterranean winds and the physical processes involved, going from pressure-driven phenomena on larger scales, to winds channeled in valleys, straits, and mountain gaps. Close to the ground, the effects of the terrain and

surface on turbulence influence all discussed winds. Section 5 discusses the differences between models included in this review with respect to parameterizations of those features. Furthermore, the present status of simulations and models is discussed. The last section gives a conclusion and outlook on open issues and future work.

## 2. Regional Winds

Regional winds are caused by pressure gradients on a synoptic scale in combination with local Orography and extend over several hundreds of kilometers. Many of these winds have widely known names. Mistral, Tramontane, and Cierzo owe their characteristics to channeling in inclined valleys, Bora crosses the Dinaric Alps, and the Etesians cross the Aegean Sea with many islands (Figure 1).

### 2.1. Winds Channeled in Valleys

The Rhône Valley and the Aude Valley between the Alps, the Massif Central, and the Pyrenees feature constrictions. Therefore, they cause channeling of the local winds. These winds are the Mistral (Rhône Valley) and the Tramontane (Aude Valley) and are indicated by the arrows in Figure 2. They often occur together because they happen due to similar synoptic situations during which a pressure gradient along the valleys causes Mistral and Tramontane to enter the valleys. This pressure gradient can be caused by, e.g., high pressure above the Bay of Biscay and a low-pressure system in the Gulf of Genoa [12].

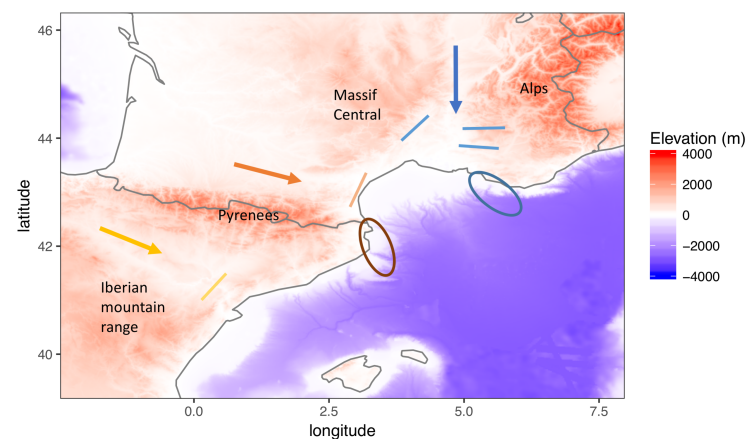


**Figure 2.** Orography and bathymetry [11] of Mistral, Tramontane, and Cierzo area (m). The arrows indicate Mistral (blue), Tramontane (orange), and Cierzo (yellow). The oval shape marks the area of highest wind speed underestimation in simulations [13]. The light lines show areas of hydraulic jumps observed by [14–16].

The air flows from high pressure (at the valley entrance) to low pressure (at the valley exit) and further accelerates due to the inclination of the valleys. Close to the coast, both winds interact with the sea breeze [7,17], see Section 3.1. The flow becomes quasi-geostrophic over the Gulf of Lion, where Coriolis force comes into play in addition to the pressure-gradient force [18]. For a geostrophic flow, the wind would travel parallel to the isobars, only influenced by pressure gradient force and Coriolis force. Due to friction at the ocean surface, the wind does not follow the isobars perfectly and thus becomes quasi-geostrophic. Both Mistral and Tramontane extend several hundreds of kilometers over the Mediterranean Sea and can even reach the African coast.

In addition to this large-scale pattern, Mistral and Tramontane show several small-scale features, which are challenging to reproduce in simulations. At constrictions, e.g., valleys, the wind speed increases due to the Venturi effect. The resolution of the simulation determines the representation of the valleys. Therefore, the simulated acceleration of the wind due to channeling also depends on the resolution of the simulation. Several kilometers

downstream of the constrictions, hydraulic jumps occur, and the wind speed drops while the flow depth increases due to a transition from a tranquil fast flow to turbulent flow (lines in Figure 2). Hydraulic jumps occur where the Rhône Valley widens [16] and behind a hill in the Aude Valley [15]. Mount Lozerè in the Massif Central causes a hydraulic jump with a wake that separates Mistral and Tramontane flows [19]. Additionally, the wall attachment or Coandă effect could cause the Mistral to stay attached to the Alps rather than being deflected to the west [20].

Med-CORDEX RCMs with grid spacings of 50 km and smaller reproduce Mistral and Tramontane wind patterns observed by satellite in general, but underestimate the wind speed, especially at the borders of the main flow (oval shapes in Figure 2) [13]. This hints at an imperfect representation of the Coandă effect in the simulations. RCMs with smaller grid spacing showed higher wind speeds and a better agreement with the observations. Modifying the roughness length parameterization can further improve the Mistral and Tramontane wind field over the Mediterranean Sea [21]. Idealized studies showed that increasing the orographic resolution can improve the simulation of Mistral and Tramontane wind fields more than parameterizations of the subgrid-scale orography [22]. In future climate conditions, Tramontane is predicted to occur less frequently while the number of Mistral days per year does not change significantly in projections with both GCMs and Med-CORDEX RCMs [23].

Cierzo is a northwesterly wind occurring in the Ebro Valley in Spain caused by synoptic conditions similar to those of Mistral and Tramontane. It is a cold, dry, and gusty wind [24]. In contrast to the strongly constricting valleys which channel Mistral and Tramontane, the Ebro Valley opens to the Mediterranean Sea with a triangular shape between the Pyrenees in the north and the Iberian mountain range in the south-west. A probable location of a hydraulic jump lies about 60 km downwind of Zaragoza (yellow line in Figure 2) [14]. In the Ebro Valley, a second local wind occurs; the warm and moist southeastern Bochorno [25].

Another wind caused by large-scale pressure patterns in combination with local orography is the Vardaris in the Axios Valley in Greece. A simulated Vardaris episode using an RCM with 20 km, 5 km, and 1 km nesting showed good agreement with the observed wind speed [26]. Small-scale features—such as a wake in the lee of a mountain—were present in the simulation. However, the simulation only covered one day and it is stressed that simulations covering longer periods are necessary for a deeper understanding of Vardaris [26].

An east–west pressure gradient can cause an easterly wind named Koshava in the Danube Valley between the Southern Carpathians and the Balkan Mountains [27]. It is channeled in narrow valleys and shows characteristics of mountain gap flows.

## 2.2. Bora

Bora is a gusty downslope windstorm in the Adriatic region with wind speeds surpassing 20 m/s and gusts up to 70 m/s. It is caused by a low-pressure system over the Adriatic Sea or a high-pressure system over central Europe—sometimes both together [10]. It lasts up to several days and is more frequent and stronger during the winter. A review of the mesoscale and microscale properties of Bora events can be found in [10]. They discuss the change of Bora interpreted as a katabatic flow, which is valid for weak Bora events and the early and late stages of Bora events to a downslope windstorm, especially for strong Bora events. Furthermore, they describe several types of Bora winds: The ‘Dark Bora’ that shows clouds and is not as abundant as the ‘Clear Bora’ without clouds, the ‘Deep Bora’ that reaches up throughout the troposphere and is on average weaker than the ‘Shallow Bora’. They also mention that mountain gap flows occur during Bora events and orographic wave breaking determines the Bora intensity. The strongest surface winds belong to the Bora shooting flow in the lowest 1 km below the primary wave breaking region.

A case study on Bora events showed that a grid spacing of 3 km is sufficient for the reproduction of observed Bora wake structures [10]. When comparing two RCM

simulations with 2.8 and 12 km grid spacing, gap winds were present in both simulations, but only the 2.8 km simulation featured wave breaking [28], which is in agreement with the aforementioned study. A study about winds in the Adriatic region in several EURO-CORDEX RCMs with 0.11° grid spacing found a decrease in Bora events during winters in the 21st century [29]. Further studies on Bora could enhance the understanding of air-sea interactions, the role of islands, as well as the influence of Coriolis force [10].

### 2.3. Etesians/Meltemi

The Etesians are northerly winds in the Aegean Sea, mostly during summer and early autumn. These winds are also called Meltemi. They are associated with a high-pressure system over the Balkans and a thermal low over the Middle East leading to a strong east-west surface pressure gradient [30,31]. The deepening of the thermal low over the Middle East during the day explains the fact that the Etesians usually get more intense in the afternoon. The Etesians are a phenomenon on a large spatial scale, sometimes characterized as monsoonal type winds [30]. At the Greek and Turkish shores of the Aegean Sea, high mountains confine the low-level flow of the Etesians. Due to the complex orography of the Aegean Sea with many islands of different sizes, the Etesians show a complex wind pattern, including channeling effects in straits and mountain gaps.

A study of the Etesians in several EURO-CORDEX RCMs with 12 km grid spacing found that most RCMs reproduce the number of Etesian days, the duration of Etesian episodes, and the wind field over the Aegean Sea better than the driving model [32]. The large-scale flow of the Etesians can be reproduced in an RCM with 2.8 km and 50 km grid spacing, but 2.8 km simulations performed better in terms of small-scale features—especially in the wind direction around islands [33].

### 2.4. Scirocco, Ghibli, and Khamsin

Dry and warm southerly or southeasterly winds occur along the Mediterranean coast of Africa and go by many names, e.g., Scirocco, Ghibli, and Khamsin. These winds transport continental tropical air from the warm sector of eastward-moving depressions. They occur mainly during spring but also during autumn when the depressions move south of the Mediterranean Sea [34]. The air originating from that area is hot, dusty, and dry. It can cause severe sandstorms. When the air masses reach Italy, they bring Saharan dust and dirty snow.

Many of the regional winds are relatively cold and dry, such as Mistral, Tramontane, Bora, and Etesians. Those winds have been studied with simulations over long periods and with several resolutions. Their overall wind patterns are well represented in simulations with grid spacings of about 12–25 km. However, smaller grid spacings are necessary for a good representation of small-scale features such as wave breaking. Fewer studies exist on the dry and warm winds along the Mediterranean coast of Africa.

## 3. Local Wind Systems with Diurnal Cycles

The local temperature and pressure differences undergoing a diurnal cycle cause winds between land and sea areas as well as between valleys and plains close to mountain ranges.

### 3.1. Sea Breeze and Land Breeze

Sea breezes develop due to a pressure gradient between the air above the sea and the air above the land. When the land surface temperatures increase during the day, a thermal low develops over land. Due to the larger heat capacity of water, the sea surface temperature shows a less pronounced diurnal cycle. The air closely above the sea surface flows in the direction of the thermal low, i.e., a sea breeze develops during the day [17]. During the night, the land surface cools. Thus, a thermal high develops, which causes the wind to change direction—a land breeze occurs. A review of sea breeze development and types can be found in [35]. Sea breezes extend up to about 100 km inland. Their extension over the sea is evident in satellite observations with 25 km grid spacing [36]

but has a too-small spatial extent to be investigated in GCMs [37]. Therefore, sufficient simulations of sea breezes need RCMs with 25 km or better even smaller grid spacing because to properly simulate a feature it needs to be several grid points wide.

The interaction between Mistral and sea breeze has been studied using an interactively nested simulation with a 3 km grid spacing in the Rhône Valley Delta [7]. They found in a case study that the onset of a Mistral event prevented the sea breeze from penetrating more than 40 km inland. Furthermore, they discussed how sea breeze and Mistral occurring at the same time prevent pollution to be transported away from the densely populated Marseilles area and emphasize the need for high-resolution simulations to achieve reliable and accurate predictions for such events. The sea breeze in the Gulf of Lion was studied with a coupled RCM at 20 km grid spacing [37]. It was able to reproduce the intensity, direction, and inland penetration with 5 to 20% accuracy.

Over the Adriatic Sea, a sea breeze can develop that interacts with Bora events. The interaction between the weaker summer Bora and the sea breeze was surveyed in a case study [9]. They used a two-way nested simulation with a grid spacing of 9 km over the Adriatic region, 3 km over Croatia, and 1 km over the Istrian Peninsula. The sea breeze is limited in its horizontal extent by the Bora, similar to what was observed for Mistral by [7] and shows enhanced frontogenesis. Unlike the interaction of sea breeze and Mistral, the Bora modifies the sea breeze only a little in its vertical extent. The wind pattern over the Adriatic Sea drives the sea circulation and the formation of small-scale eddies on the surface currents [9]. They also found that convection over one island obstructs the strength of Bora. In the wake of another island, they observed an onshore flow created by a rotor in the lee of a mountain.

Sea breezes also occur in other Mediterranean locations and interact with the local wind systems and were studied, e.g., in the Jordan Rift Valley [38]. The interaction with sea breeze and convection and how the sea breeze impacts thunderstorms were studied along the east coast of the Iberian Peninsula using a hydrostatic RCM with 0.025° grid spacing [39]. They found that the model resolution impacts the location and strength of sea breeze fronts. Increasing the spatial and vertical resolution also seemed to be favorable.

### 3.2. Valley Winds

Due to differences in solar radiation and heating of the air, a diurnal wind system develops in valleys. During the day, the wind blows up-valley, while, at night, it flows down-valley. This wind system extends over smaller scales—depending on the valley—than regional winds. Such winds are, therefore, more difficult to represent correctly in simulations. Valley wind systems occur in all areas of the Mediterranean that feature valleys, e.g., the Adige Valley in the Italian Alps [40]. Interactions between valley winds and regional winds are still to be investigated in RCMs.

The sea breeze and its interactions with Mistral and Bora have been studied using high-resolution simulations. In contrast to the sea breeze, the land breeze was not studied in such detail. Many valleys exist in the Mediterranean and, therefore, many valley wind systems. Most of them were not yet studied in RCMs, due to their large number and the high resolution needed.

## 4. Channeling in Straits

Straits are narrow passages of water that connect two larger bodies of water. The most widely known straits in the Mediterranean Region (from west to east) are (gray circles in Figure 1):

- the Strait of Gibraltar between Europe and Africa, which connects the Mediterranean Sea to the Atlantic Ocean;
- the Strait of Bonifacio between Corsica and Sardinia connecting the Tyrrhenian Sea from the Gulf of Lion;
- the Strait of Messina between Sicily and Calabria connecting the Tyrrhenian Sea to the Ionian Sea.

The Mediterranean Sea connects to the Sea of Marmara through the Dardanelles and further to the Black Sea by the Bosphorus. Since the Mediterranean Sea features many islands, a large number of straits exist between the islands and between islands and larger land bodies. This makes channeling in straits an abundant and important phenomenon in the Mediterranean area.

Straits force passing air masses to accelerate due to the Venturi effect. This can cause gusty winds that are hazardous to structures on land and ships that travel the straits or the open sea in their vicinity. Consequently, they are important to the local population and often given specific names. Many simulation studies are dealing with ocean circulation within straits, which also show interactions with wind patterns, e.g., [41–47]. Among the in-depth studied winds in straits are those of the Strait of Gibraltar and the Strait of Bonifacio.

#### 4.1. Strait of Gibraltar

The Strait of Gibraltar extends from east to west and is about 20 km wide at its narrowest point. It shows 1000–2000 m high orography on both sides (see Figure 3). Therefore, the channeling of winds induced by synoptic or local scale pressure gradients is strong [48]. Two winds occur in the strait, the easterly Levanter and the westerly Poniente (also named Vendaval).

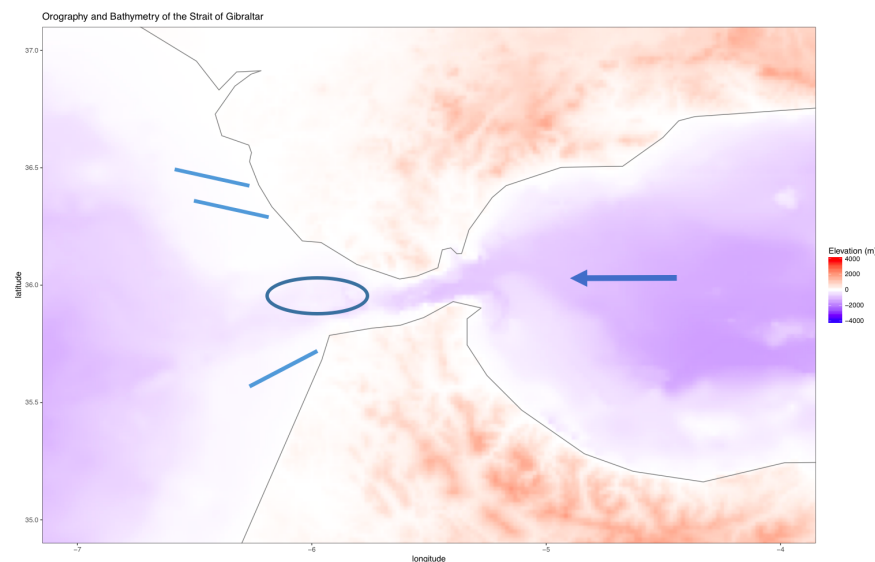


**Figure 3.** Orography and bathymetry [11] of the Strait of Gibraltar (m). The arrow indicates the Levanter wind. The oval shape marks the area of highest wind speeds during Levanter events and the light blue lines show areas of high wind speeds found by [8].

Two groups of easterly Levanter winds, synoptic-scale and mesoscale events, can be observed [49]. The synoptic-scale events show a large westward extension into the Atlantic Ocean and an upward extension into the upper troposphere. Within the strait they are geostrophic. The mesoscale Levanters occur directly in the strait in conjunction with a mesoscale surface low west of the narrowest point. These ageostrophic mesoscale Levanters occur mainly during summer and reach only about 1000 m high. They show the highest velocities near Tangier, i.e., leeward of the narrowest spot of the strait (dark blue oval shape in Figure 3), hinting at an effect in addition to the Venturi effect. This observation could be explained by the small upstream Froude number of mesoscale Levanters which causes most of the upstream air to be funneled through the strait, while the airflow up above the strait experiences partial blocking and some flow over the topography [49]. In the lee, this air is heated adiabatically. Furthermore, the only weak drag above water and the acceleration of the low-level winds cause a divergence over the coast and force the air to descend. In combination with subsidence heating, a mesoscale surface-low develops in the western region of the strait and further enhances the mesoscale Levanters.

A Levanter simulation using a non-hydrostatic weather prediction model with 1 km grid spacing in two case studies, indicates that an inversion plus the Venturi effect could cause the observed wind speed patterns [8]. Bands of high wind speed were present west of the strait in the simulation as well as in satellite pictures of the same dates (indicated by light blue lines in Figure 3). The bands need further examination and hint that a high spatial resolution is necessary to simulate Levanter events.

Fewer studies dealt with westerly Poniente/Vendaval. Both winds interact with the surface water which is exchanged between the Mediterranean Sea and the Atlantic through the strait. This makes them interesting for coupled ocean–atmosphere simulations [42]. Furthermore, an evaluation of the winds in the Strait of Gibraltar in a climate context is still missing.

#### 4.2. Strait of Bonifacio

The Strait of Bonifacio is east–west oriented between the islands Corsica and Sardinia and about 10 km wide. Two main winds occur, the westerly Libeccio and the easterly Gregale. Libeccio occurs during all seasons and shows wind speeds larger than 8 m/s, while Gregale occurs during winter and shows smaller wind speeds of 5 to 8 m/s [44]. Mistral events, which extend over the whole Gulf of Lion and reach the Strait of Bonifacio can also appear as a Libeccio [50].

Several studies dealt with the ocean currents and waves in the strait and emphasized the importance of wind data because the wind is the main driving factor for surface currents and waves [43–45]. An evaluation for two Libeccio cases with 2.8 km grid spacing simulations with scatterometer data found that the simulations reproduce the Libeccio jet in general [51]. An easterly Gregale event, too, was identified in the observation data combined with a Tramontana wind coming from the Po valley in Italy.

#### 4.3. Other Straits

Many more straits exist in the Mediterranean region. Some of them are rather broad but show increased wind speed due to channeling effects [52]. In some straits, the ocean circulation was surveyed in-depth, i. a. the Strait of Messina between Sicily and the Italian mainland [42,46,47] and the Strait of Otranto between Italy and Albania [41].

In the broader straits such as, e.g., the Sicily Channel between Sicily and Africa, the general ocean circulation has more impact on the local ocean currents than the local wind within the strait [42]. This indicates that the wind situation over the surrounding water bodies can pose a relevant influence on the ocean current in the broader straits and could be taken into consideration when defining the simulated domain.

In the eastern Mediterranean many small islands and straits exist, e.g., the Strait of Corfu and the Strait of Ithaca in the Ionian Sea. In the Aegean Sea, many straits exist, e.g., the Chios Strait, Euripus Strait, Mycale Strait, and Mytilini Strait. Due to their small spatial extent, only very high-resolution simulations can simulate the wind and ocean circulation in these areas.

Among the straits studied in great detail are the Strait of Gibraltar and the Strait of Bonifacio. The many Mediterranean islands feature many more straits which probably are a rewarding subject for further studies. High-resolution and coupled RCMs could be used to investigate the interaction between the wind channeled in the straits and the ocean currents in a climate context.

#### 4.4. Mountain Gap Flows

Wind channeling can also occur in gaps between mountains, both in a mountain range such as the Alps or the Massif central and at islands. Since the orography within a mountain gap is not flat (in contrast to the sea surface in a strait), the flow through a mountain gap shows also other effects than that through a strait. Here, only two mountain gap flows are discussed, even though many more are present in the Mediterranean area.



The gap between Crete’s two highest mountains, Lefka Ori and Idi is about 30 to 40 km wide and 23 km long, with a complex orography within the gap. A northerly flow intensification due to channeling in the mountain gap was identified in a simulation with a 1 km grid spacing [30]. The Koshava between the Southern Carpathians and the Balkan Mountains crosses four small gaps and is also characterized as a mountain gap flow [27]. Mountain gap flows are abundant in the Mediterranean area and require high-resolution simulations, similar to the valley winds discussed above.

### 5. Differences between Models

Since models are a simplification of reality, they use parameterizations for processes they can not resolve. The choices on how these simplifications are carried out vary between the models and thus cause possibly large differences between simulations with similar or even identical input data, but different models.

For the local population and structures, the wind close to the ground has the biggest impact. It is usually referred to as winds 10 m above the ground. Here, the wind is strongly influenced by friction due to earth/sea surface roughness. Figure 4 shows 10 m wind on a day with a Mistral as simulated with several models (upper three rows), ERA-Interim reanalysis [53], and observation data sets QuikSCAT [54] and SAFRAN [55,56] (bottom row) [57]. In this figure the panels are named as institution–model followed by grid spacing in °. The scale shown in the last panel applies to all panels and gives the 10 m wind in m/s.

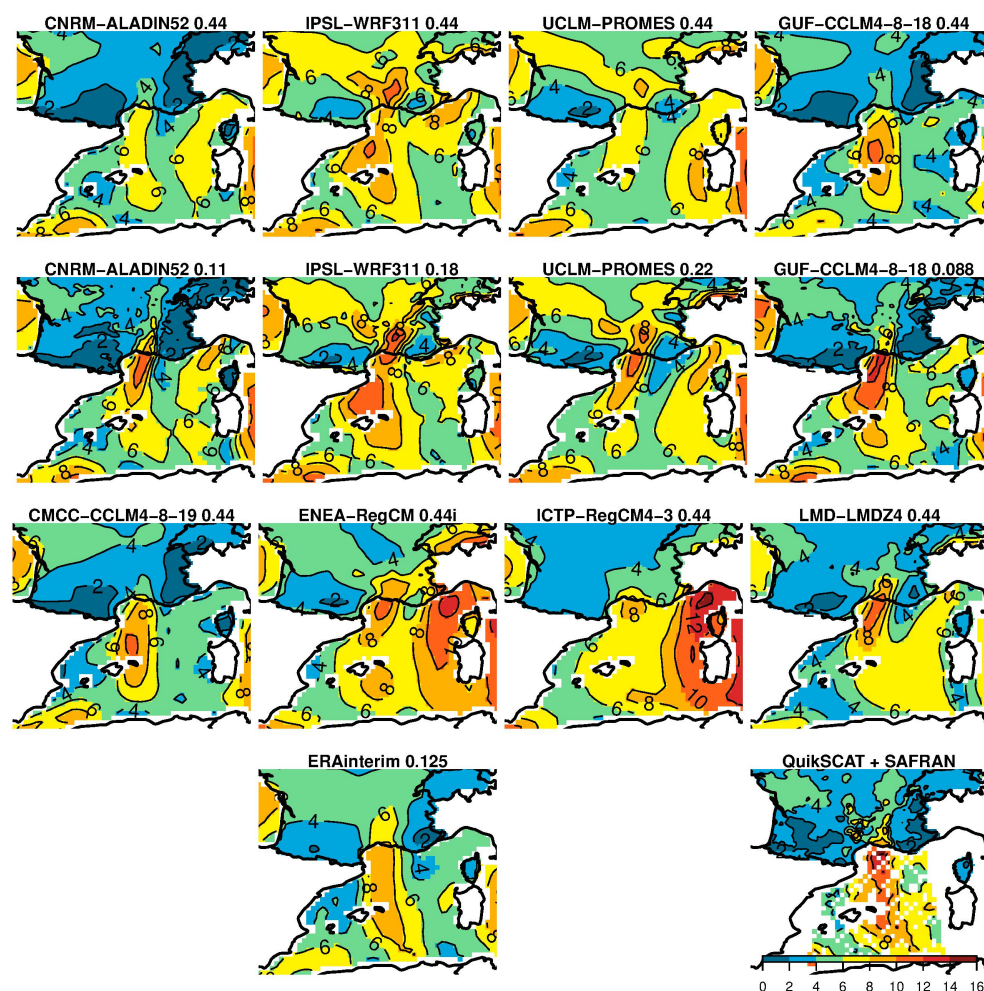


**Figure 4.** Daily mean 10 m surface wind speed (m/s) on 24 March 2002 obtained from Med-CORDEX RCMs [5], ERA-Interim [53], QuikSCAT [54], and SAFRAN [55,56]. The color scale in the last panel applies to all panels. Figure from [57].

Even though all simulations shown in Figure 4 are driven by ERA-Interim and thus had the same boundary conditions, the simulated wind fields for this day vary. While some simulations can capture the overall Mistral pattern on that day—and on average during Mistrals events [21]—others show low wind speed in the Mistral area. Furthermore, models with two simulations on different grid spacings (row one and two) show higher wind speeds in simulations with smaller grid spacing, i.e., simulations with higher resolution. This resolution-dependent change in wind speed improves the simulation of Mistral events, because simulations tend to underestimate the wind speed during such events [21].

Since the lowest model level of RCMs usually is chosen to be located at a greater height, the 10 m wind is calculated using parameterizations including surface properties; especially the roughness length. Above the land surface, the roughness length is selected to match the local structures—such as forests, crops, buildings—and the subgrid-scale orography, which was shown to impact simulated Mistral and Tramontane wind patterns [22]. Both cannot be resolved by the RCM and need to be parameterized. Above the sea surface, the sea state—e.g., waves, swell, and white capping—is indicative of the surface roughness but is also based on the local winds, which cause waves. Many RCMs use the Charnock parameterization [58] or one of its variants to include this relationship. The parameterization of sea surface impacts the wind pattern of Mistral and Tramontane [13] and thus probably also other mesoscale winds above the sea surface.

Planetary boundary layer (PBL) parameterizations impact the way how energy is transported vertically and thus how the information about the Earth’s surface impacts the higher levels of the simulation. An overview of several common PBL parameterization schemes is given in [59]. Table 1 shows the PBL schemes used in the models of the studies discussed in this review.

**Table 1.** Properties of the RCMs (atmosphere component) included in the studies.

| Model     | (Non-)Hydrostatic | PBL                            | Studies                |
|-----------|-------------------|--------------------------------|------------------------|
| ALADIN    | both options [60] | Louis [61]                     | [21,29,32]             |
| AROME     | non-hydrostatic   | Cuxart [62]                    | [18]                   |
| ARPEGE    | both options [60] | Ricard and Royer [63]          | [32]                   |
| COSMO-CLM | non-hydrostatic   | Mellor-Yamada [64]             | [13,21–23,28,29,33,51] |
| HIRHAM    | hydrostatic       | Louis [61]                     | [29,32]                |
| HIRLAM    | hydrostatic       | Cuxart [62]                    | [39]                   |
| LMDZ      | hydrostatic       | Mellor-Yamada [64]             | [21]                   |
| Méso-NH   | non-hydrostatic   | BouLac [65]                    | [7]                    |
| MM5       | non-hydrostatic   | MRF [66]                       | [16,30]                |
| PERIDOT   | hydrostatic       | BouLac [65]                    | [14]                   |
| PROMES    | hydrostatic       | Cuxart [62]                    | [21]                   |
| QBOLAM    | hydrostatic       | Cuxart [62]                    | [52]                   |
| RACMO22E  | hydrostatic       | Meijgaard [67]                 | [29]                   |
| RCA4      | hydrostatic       | Cuxart [62]                    | [29,32]                |
| RegCM     | hydrostatic       | Holtslag [68], UW-PBL [69]     | [23,29]                |
| REMO      | non-hydrostatic   | Louis [61], Mellor-Yamada [64] | [29]                   |
| UM        | non-hydrostatic   | [70]                           | [8]                    |
| WRF       | non-hydrostatic   | YSU [71]                       | [9,21,26,32,37]        |

## 6. Summary and Outlook

In this review, several Mediterranean mesoscale wind systems and associated processes are discussed. The focus is on the challenges for simulations with regional climate models. The findings are summarized under the four questions raised in the introduction.

For which winds do high-resolution simulations exist and do they provide additional insights? Table 2 shows the studies discussed in this review according to the wind system and simulation grid spacing. High-resolution simulations were used, i.e., for the regional winds Mistral, Bora, and Etesians. Land breeze and sea breeze channeling in straits and mountain gap flows also were studied in high-resolution simulations. The added value of high-resolution simulation was shown for wave breaking in Bora, a better representation of

sea breeze and its interaction with other wind systems, and small scale wind features as mountain gap flows, channeling in straits, and flow around islands.

**Table 2.** Studies included in this review. The column ‘Other Studies’ includes idealized and ocean only studies, as well as reviews and process studies.

| Location                        | Wind System         | RCM Grid Spacing |          | Other Studies |
|---------------------------------|---------------------|------------------|----------|---------------|
|                                 |                     | ≈12–25 km        | ≈1–3 km  |               |
| <b>Regional Winds</b>           |                     |                  |          |               |
| Rhone Valley                    | Mistral             | [13,18,21,23]    | [7,16]   | [12,19,20,22] |
| Aude Valley                     | Tramontane          | [13,18,23]       |          | [12,15,22]    |
| Ebro Valley                     | Cierzo              | [14]             |          | [24]          |
| Ebro Valley                     | Bochorno            |                  |          | [25]          |
| Axios Valley                    | Vardaris            |                  | [26]     |               |
| Adriatic region                 | Bora                | [28,29]          | [10,28]  | [10]          |
| Aegan Sea                       | Etesians/Meltemi    | [32]             | [30,33]  | [31]          |
| Coast of Africa                 | Scirocco, Ghibli... |                  |          | [34]          |
| Danube Valley                   | Koshava             |                  |          | [27]          |
| <b>Winds with diurnal cycle</b> |                     |                  |          |               |
| Coast                           | Sea/land breeze     | [18,37]          | [7,9,39] | [17,35,36,38] |
| Valleys                         | Valley winds        |                  |          | [40]          |
| <b>Channeling in Straits</b>    |                     |                  |          |               |
| Gibraltar                       | Levanter/Poniente   |                  | [8]      | [52]          |
| Bonifacio                       | Libeccio/Gregale    |                  | [51]     | [42,48,49]    |
| Messina                         |                     |                  |          | [42,46,47]    |
| Sicily channel                  |                     |                  |          | [42]          |
| Otranto                         |                     |                  |          | [41]          |
| <b>Mountain gap flows</b>       |                     |                  |          |               |
| Crete                           |                     |                  | [30]     |               |
| Danube Valley                   | Koshava             |                  |          | [27]          |

Which Mediterranean wind systems have already been studied in detail, and which wind systems have only little data available and appear promising for further study? The relatively cold and dry regional winds of the Mediterranean, such as Mistral, Tramontane, Bora, and Etesians have been investigated extensively on different resolutions and over long time scales. Additionally to very high-resolution studies on those winds, many less widely known winds could be studied such as the winds called Tramontana in different parts of the Mediterranean area. The relatively warm and moist regional winds, e.g., Scirocco, Ghibli, and Bochorno, are also promising for future studies.

Winds on smaller spatial scales, such as winds in straits, valleys, and mountain gaps, mostly were studied in case studies, but not yet in climate simulations. Well-studied straits with case studies include the Straits of Gibraltar, Bonifacio, and Messina. However, there are many more straits in the Mediterranean area that still have to be studied. The same is true for valley winds and mountain gap flows—only a small fraction of those were already studied, e.g., in Crete and in the Adriatic region. Since several mountain ranges exist in the Mediterranean region this leaves space for further research—also for the interaction of winds on a larger scale and mountain gaps. The interaction between small-scale winds and the ocean in coupled climate simulation also could give further insight and be interesting for ship traffic and wave modeling.

Which grid spacing is needed to resolve phenomena such as gap winds, sea breeze, and wave breaking? Table 3 gives an overview of resolved phenomena depending on grid spacing. GCMs and RCMs with about 50 km grid spacing represent winds on larger scales quite well. In general, they can reproduce the dates of wind systems induced by large-scale pressure patterns such as Mistral, Tramontane, and Etesians. Simulations with grid spacings of about 12–25 km reproduce the wind speed and wind direction patterns even better, e.g., gap flows during Bora events. These RCM simulations with grid spacings

of 12 km and above were also used in climate projection studies to estimate the future development of Mistral, Tramontane, and Etesians.

The simulation of winds in narrow straits and mountain gaps requires even higher resolutions, as does the simulation of small-scale features in regional winds, e.g., wave breaking during Bora. Small-scale features in the wind patterns arise in simulations with grid spacings of 1–3 km. Since these simulations are computationally expensive, most studies discussed here included only a short period and a small area, e.g., a single strait.

**Table 3.** Resolved phenomena and grid spacing for each simulation type: global circulation models (GCM), regional climate models (RCM), and convection permitting simulations (CPS).

| Resolved Phenomena   | Simulation Type     | Grid (km) |
|--|---------------------|-----------|
| large scale sea level pressure patterns driving regional winds   | GCM                 | ≈100      |
| regional wind patterns   | RCM low resolution  | ≈50       |
| regional wind patterns improved, gap winds, sea breeze   | RCM high resolution | ≈12–25    |
| small scale features, sea breeze improved, wave breaking, flow around islands, channeling in straits, narrow mountain gaps | CPS                 | ≈1–3      |

Which model improvements—besides higher resolution—are needed? Of high importance for surface wind simulations is the sufficient simulation of surface properties, e.g., through the surface roughness length. Since ocean circulation interacts with the local and regional wind, a good representation of small-scale wind fields is also necessary for ocean simulations with high resolution. Coupled models can simulate the interactions between the air and the sea and add important improvements in Mediterranean Sea simulations. Here, several improvements are possible, including more information about the sea state, e.g., by using a wave model. Future work will show how well even small features, e.g., in straits and around islands, can be resolved both in the atmosphere and ocean and thus help to discover more interesting aspects of mesoscale winds.

Studies with very high-resolution simulations often cover only a small area or period due to limited computational resources. High-resolution simulations over larger areas or even the whole Mediterranean area could make studying interactions between small-scale phenomena in different areas feasible. Furthermore, they could improve the simulation of interactions between winds already well represented in coarser simulations and the small-scale phenomena, e.g., between Mistral and sea breeze or between Etesians and channeling in straits or the flow around islands. Additionally, they could reveal possible connections and interactions between distant small-scale phenomena such as the winds in the Strait of Gibraltar and winds in the Strait of Bonifacio or the Sicily Channel.

With increasing computational resources, longer simulations with larger spatial coverage and higher resolution become feasible and interaction between winds in the whole Mediterranean region on different spatial and time scales becomes possible to simulate and understand. This will advance our knowledge of the small-scale wind fields in the entire Mediterranean region, especially in its various straits, mountain gaps, and valleys.

Furthermore, climate simulations with such small grid spacings will improve the confidence in how well the small-scale features are reproduced and which changes in future climate conditions can be expected. Since the Mediterranean area is expected to experience a strong impact of climate change, this information is valuable for further studies on risk, adaptation, and mitigation, e.g., for ship traffic.

Additionally, coupled simulations add more information about the sea state to the simulation of mesoscale winds. Coupled climate simulations with high resolution would add more knowledge on the interaction between atmosphere and ocean and the role of winds in the climate system.

**Funding:** This research was funded by the European Union’s Horizon 2020 research and innovation programme under grant agreement No 776661 (SOCLIMPACT) and the German Federal Ministry of Education and Research (BMBF) under grant MiKliP II (FKZ 01LP1518C).

**Institutional Review Board Statement:** Not applicable.

**Informed Consent Statement:** Not applicable.

**Data Availability Statement:** Not applicable.

**Conflicts of Interest:** The author declares no conflict of interest.

## Abbreviations

The following abbreviations are used in this manuscript:

|             |   |
|-------------|---|
| CORDEX      | coordinated regional climate downscaling experiment |
| CPS         | convection permitting simulations                   |
| EURO-CORDEX | European CORDEX                                     |
| GCM         | global circulation model                            |
| Med-CORDEX  | Mediterranean CORDEX                                |
| PBL         | planetary boundary layer                            |
| RCM         | regional climate model                              |

## References

- Giorgi, F. Climate change hot-spots. *Geophys. Res. Lett.* **2006**, *33*, 1–4. [[CrossRef](#)]
- Diffenbaugh, N.S.; Giorgi, F. Climate change hotspots in the CMIP5 global climate model ensemble. *Clim. Chang.* **2012**, *114*, 813–822. [[CrossRef](#)] [[PubMed](#)]
- Giorgi, F.; Jones, C.; Asrar, G.R. Addressing climate information needs at the regional level: The CORDEX framework. *World Meteorol. Organ. Bull.* **2009**, *58*, 175–183.
- Giorgi, F.; Gutowski, W.J. Regional Dynamical Downscaling and the CORDEX Initiative. *Annu. Rev. Environ. Resour.* **2015**, *40*, 467–490. [[CrossRef](#)]
- Ruti, P.M.; Somot, S.; Giorgi, F.; Dubois, C.; Flaounas, E.; Obermann, A.; Dell’Aquila, A.; Pisacane, G.; Harzallah, A.; Lombardi, E.; et al. Med-CORDEX initiative for Mediterranean climate studies. *Bull. Am. Meteorol. Soc.* **2016**, *97*, 1187–1208. [[CrossRef](#)]
- Jacob, D.; Petersen, J.; Eggert, B.; Alias, A.; Christensen, O.B.; Bouwer, L.M.; Braun, A.; Colette, A.; Déqué, M.; Georgievski, G.; et al. EURO-CORDEX: New high-resolution climate change projections for European impact research. *Reg. Environ. Chang.* **2014**, *14*, 563–578. [[CrossRef](#)]
- Bastin, S.; Drobinski, P.; Caccia, J.L.; Campistron, B.; Dabas, A.M.; Delville, P.; Reitebuch, O.; Werner, C.; Garde, L. On the interaction between the sea breeze and a summer Mistral event at the exit of the Rhône valley. *Mon. Weather Rev.* **2006**, *134*, 1647–1668. [[CrossRef](#)]
- Capon, R.A. High resolution studies of the Gibraltar Levanter validated using sun-glint anemometry. *Meteorol. Appl.* **2006**, *13*, 257–265. [[CrossRef](#)]
- Prtenjak, M.T.; Viher, M.; Jurković, J. Sea-land breeze development during a summer bora event along the north-eastern Adriatic coast. *Q. J. R. Meteorol. Soc.* **2010**, *136*, 1554–1571. [[CrossRef](#)]
- Grisogono, B.; Belušić, D. A review of recent advances in understanding the meso- and microscale properties of the severe Bora wind. *Tellus Ser. A Dyn. Meteorol. Oceanogr.* **2009**, *61*, 1–16. [[CrossRef](#)]
- Amante, C.; Eakins, B.W. *ETOPO1 1 Arc-Minute Global Relief Model: Procedures, Data Sources and Analysis*; National Geophysical Data Center: Boulder, CO, USA, 2009; Volume 10, p. V5C8276M. [[CrossRef](#)]
- Jacq, V.; Albert, P.; Delorme, R. Le mistral. *La Météorol.* **2005**, *50*, 30–38.
- Obermann, A.; Edelmann, B.; Ahrens, B. Influence of sea surface roughness length parameterization on Mistral and Tramontane simulations. *Adv. Sci. Res.* **2016**, *13*, 107–112. [[CrossRef](#)]
- Masson, V.; Bougeault, P. Numerical Simulation of a Low-Level Wind Created by Complex Orography: A Cierzo Case Study. *Mon. Weather Rev.* **1996**, *124*, 701–715. [[CrossRef](#)]
- Drobinski, P.; Flamant, C.; Dusek, J.A.N.; Flamant, P.H.; Pelon, J. Observational evidence and modelling of an internal hydraulic jump at the atmospheric boundary-layer top during a Tramontane event. *Bound. Layer Meteorol.* **2001**, *98*, 497–515. [[CrossRef](#)]
- Drobinski, P.; Bastin, S.; Guenard, V.; Caccia, J.L.; Dabas, A.M.; Delville, P.; Protat, A.; Reitebuch, O.; Werner, C. Summer mistral at the exit of the Rhône valley. *Q. J. R. Meteorol. Soc.* **2005**, *131*, 353–375. [[CrossRef](#)]
- Simpson, J.E. *Sea Breeze and Local Wind*; Cambridge University Press: Cambridge, UK, 1994; p. 234.
- Drobinski, P.; Alonzo, B.; Basdevant, C.; Cocquerez, P.; Doerenbecher, A.; Fourrié, N.; Nuret, M. Lagrangian dynamics of the mistral during the HyMeX SOP2. *J. Geophys. Res.* **2017**, *122*, 1387–1402. [[CrossRef](#)]

19. Guenard, V.; Drobinski, P.; Caccia, J.L.; Campistron, B.; Benech, B. An observational study of the mesoscale mistral dynamics. *Bound. Layer Meteorol.* **2005**, *115*, 263–288. [[CrossRef](#)]
20. Giles, B.D. Fluidics, the Coanda Effect, and some orographic winds. *Archiv für Meteorol. Geophys. Und Bioklimatol. Ser. A* **1977**, *25*, 273–279. [[CrossRef](#)]
21. Obermann, A.; Bastin, S.; Belamari, S.; Conte, D.; Gaertner, M.A.; Li, L.; Ahrens, B. Mistral and Tramontane wind speed and wind direction patterns in regional climate simulations. *Clim. Dyn.* **2018**, *51*, 1059–1076. [[CrossRef](#)]
22. Obermann-Hellhund, A.; Ahrens, B. Mistral and Tramontane Simulations with changing Resolution of Orography. *Atmos. Sci. Lett.* **2018**, *19*, e848. [[CrossRef](#)]
23. Obermann-Hellhund, A.; Conte, D.; Somot, S.; Torma, C.Z.; Ahrens, B. Mistral and Tramontane wind systems in climate simulations from 1950 to 2100. *Clim. Dyn.* **2018**, *50*, 693–703. [[CrossRef](#)]
24. Riosalido, R.; Vázquez, L.; Gorgo, A.; Jansà, A. Cierzo: Northwesterly wind along the Ebro Valley as a meso-scale effect induced on the lee of the Pyrenees mountain range: A case study during ALPEX Special Observing Period. *Sci. Results Alp. Exp. (ALPEX)* **1986**, *2*, 565–575.
25. Jiménez, P.A.; González-Rouco, J.F.; Montávez, J.P.; García-Bustamantea, E.; Navarro, J. Climatology of wind patterns in the northeast of the Iberian Peninsula. *Int. J. Climatol.* **2009**, *29*, 501–525. [[CrossRef](#)]
26. Koletsis, I.; Giannaros, T.M.; Lagouvardos, K.; Kotroni, V. Observational and numerical study of the Vardaris wind regime in northern Greece. *Atmos. Res.* **2016**, *171*, 107–120. [[CrossRef](#)]
27. Romanić, D.; Čurić, M.; Lompar, M.; Jovičić, I. Contributing factors to Koshava wind characteristics. *Int. J. Climatol.* **2016**, *36*, 956–973. [[CrossRef](#)]
28. Josipović, L. Die Bora an der kroatischen Adria–Schwerewellenbrechen und Strömungskanalisationen in Messwerten und Modellsimulationen. Bachelor’s Thesis, Goethe Universität Frankfurt, Frankfurt, Germany, 2018; pp. 1–51.
29. Belušić Vozila, A.; Güttler, I.; Ahrens, B.; Obermann-Hellhund, A.; Telišman Prtenjak, M. Wind Over the Adriatic Region in CORDEX Climate Change Scenarios. *J. Geophys. Res. Atmos.* **2019**, *124*, 110–130. [[CrossRef](#)]
30. Koletsis, I.; Lagouvardos, K.; Kotroni, V.; Bartzokas, A. The interaction of northern wind flow with the complex topography of Crete Island - Part 2: Numerical study. *Nat. Hazards Earth Syst. Sci.* **2010**, *10*, 1845–1855. [[CrossRef](#)]
31. Dafka, S.; Xoplaki, E.; Toreti, A.; Zanis, P.; Tyrlis, E.; Zerefos, C.; Luterbacher, J. The Etesians: from observations to reanalysis. *Clim. Dyn.* **2016**, *47*, 1569–1585. [[CrossRef](#)]
32. Dafka, S.; Toreti, A.; Luterbacher, J.; Zanis, P.; Tyrlis, E.; Xoplaki, E. On the ability of RCMs to capture the circulation pattern of Etesians. *Clim. Dyn.* **2017**, *51*, 1687–1706. [[CrossRef](#)]
33. Lorenz, V. Evaluation of Etesian Simulations with the Regional Climate Model COSMO-CLM. Ph.D. Thesis, Goethe-Universität Frankfurt, Frankfurt, Germany, 2018.
34. Warner, T.T. African deserts. In *Desert Meteorology*; Cambridge University Press: Cambridge, UK, 2009; pp. 79–104.
35. Miller, S.T.; Keim, B.D.; Talbot, R.W.; Mao, H. Sea breeze: Structure, forecasting, and impacts. *Rev. Geophys.* **2003**, *41*. [[CrossRef](#)]
36. Vovk, O. Land-See- Windsysteme in Scatterometerdatensätzen. Bachelor’s Thesis, Goethe-Universität Frankfurt, Frankfurt, Germany, 2016.
37. Drobinski, P.; Bastin, S.; Arsouze, T.; Béranger, K.; Flaounas, E.; Stéfanon, M. North-western Mediterranean sea-breeze circulation in a regional climate system model. *Clim. Dyn.* **2018**, *51*, 1–17. [[CrossRef](#)]
38. Naor, R.; Potchter, O.; Shafir, H.; Alpert, P. An observational study of the summer Mediterranean Sea breeze front penetration into the complex topography of the Jordan Rift Valley. *Theor. Appl. Climatol.* **2017**, *127*, 275–284. [[CrossRef](#)]
39. Azorin-Molina, C.; Tijm, S.; Ebert, E.E.; Vicente-Serrano, S.M.; Estrela, M.J. High Resolution HIRLAM Simulations of the Role of Low-Level Sea-Breeze Convergence in Initiating Deep Moist Convection in the Eastern Iberian Peninsula. *Bound. Layer Meteorol.* **2014**, *154*, 81–100. [[CrossRef](#)]
40. Giovannini, L.; Laiti, L.; Serafin, S.; Zardi, D. The thermally driven diurnal wind system of the Adige Valley in the Italian Alps. *Q. J. R. Meteorol. Soc.* **2017**, *143*, 2389–2402. [[CrossRef](#)]
41. Zavatarelli, M.; Pinardi, N.; Zavatarelli, M.; The, N.P.; Sea, A. The Adriatic Sea modelling system: A nested approach. *Ann. Geophys.* **2003**, *21*, 345–364. [[CrossRef](#)]
42. Béranger, K.; Mortier, L.; Crépon, M. Seasonal variability of water transport through the Straits of Gibraltar, Sicily and Corsica, derived from a high-resolution model of the Mediterranean circulation. *Prog. Oceanogr.* **2005**, *66*, 341–364. [[CrossRef](#)]
43. De Falco, G.; De Muro, S.; Batzella, T.; Cucco, A. Carbonate sedimentation and hydrodynamic pattern on a modern temperate shelf: The strait of Bonifacio (western Mediterranean). *Estuar. Coast. Shelf Sci.* **2011**, *93*, 14–26. [[CrossRef](#)]
44. Gerigny, O.; Di Martino, B.; Romano, J.C. The current dynamics inside the Strait of Bonifacio: Impact of the wind effect in a little coastal strait. *Cont. Shelf Res.* **2011**, *31*, 1–8. [[CrossRef](#)]
45. Cucco, A.; Sinerchia, M.; Ribotti, A.; Olita, A.; Fazioli, L.; Perilli, A.; Sorgente, B.; Borghini, M.; Schroeder, K.; Sorgente, R. A high-resolution real-time forecasting system for predicting the fate of oil spills in the Strait of Bonifacio (western Mediterranean Sea). *Mar. Pollut. Bull.* **2012**, *64*, 1186–1200. [[CrossRef](#)]
46. Cucco, A.; Quattrocchi, G.; Olita, A.; Fazioli, L.; Ribotti, A.; Sinerchia, M.; Tedesco, C.; Sorgente, R. Hydrodynamic modelling of coastal seas: The role of tidal dynamics in the Messina Strait, Western Mediterranean Sea. *Nat. Hazards Earth Syst. Sci.* **2016**, *16*, 1553–1569. [[CrossRef](#)]

47. Battaglia, P.; Ammendolia, G.; Cavallaro, M.; Consoli, P.; Esposito, V.; Malara, D.; Rao, I.; Romeo, T.; Andaloro, F. Influence of lunar phases, winds and seasonality on the stranding of mesopelagic fish in the Strait of Messina (Central Mediterranean Sea). *Mar. Ecol.* **2017**, *38*, e12459. [[CrossRef](#)]
48. Scorer, R.S. Mountain-gap winds; a study of surface wind at Gibraltar. *Q. J. R. Meteorol. Soc.* **1952**, *78*, 53–61. [[CrossRef](#)]
49. Dorman, C.E.; Beardsley, R.C.; Limeburner, R. Winds in the strait of gibraltar. *Q. J. R. Meteorol. Soc.* **1995**, *121*, 1903–1921. [[CrossRef](#)]
50. Zecchetto, S.; De Biasio, F. Sea surface winds over the Mediterranean basin from satellite data (2000–04): Meso- and local-scale features on annual and seasonal time scales. *J. Appl. Meteorol. Clim.* **2007**, *46*, 814–827. [[CrossRef](#)]
51. Muth, L. Strömungskanalisation in der Straße von Bonifacio. Bachelor's Thesis, Goethe Universität Frankfurt, Frankfurt, Germany, 2016.
52. Lavagnini, A.; Sempreviva, A.M.; Transerici, C.; Accadia, C.; Casaioli, M.; Mariani, S.; Speranza, A. Offshore wind climatology over the mediterranean Basin. *Wind Energy* **2006**, *9*, 251–266. [[CrossRef](#)]
53. Dee, D.P.; Uppala, S.M.; Simmons, A.J.; Berrisford, P.; Poli, P.; Kobayashi, S.; Andrae, U.; Balmaseda, M.A.; Balsamo, G.; Bauer, P.; et al. The ERA-Interim reanalysis: Configuration and performance of the data assimilation system. *Q. J. R. Meteorol. Soc.* **2011**, *137*, 553–597. [[CrossRef](#)]
54. Lungu, T.; Dunbar, S.; Weiss, B.; Stiles, B.; Huddleston, J.; Callahan, P.; Shirtliffe, G.; Perry, K.L.; Hsu, C.; Mears, C.; et al. QuikSCAT Science Data Product User's Manual: Overview and Geophysical Data Products. *Jet Propuls. Lab.* **2006**, *3*, 91.
55. Vidal, J.P.; Martin, E.; Franchistéguy, L.; Baillon, M.; Soubeyroux, J.M. A 50-year high-resolution atmospheric reanalysis over France with the Safran system. *Int. J. Climatol.* **2010**, *30*, 1627–1644. [[CrossRef](#)]
56. Quintana-Seguí, P.; Le Moigne, P.; Durand, Y.; Martin, E.; Habets, F.; Baillon, M.; Canellas, C.; Franchisteguy, L.; Morel, S. Analysis of near-surface atmospheric variables: Validation of the SAFRAN analysis over France. *J. Appl. Meteorol. Climatol.* **2008**, *47*, 92–107. [[CrossRef](#)]
57. Obermann-Hellhund, A. Mistral and Tramontane : Simulation of Mesoscale Winds in Regional Climate Models. Ph.D. Thesis, Goethe-Universität Frankfurt, Frankfurt, Germany, 2017.
58. Charnock, H. Wind stress on a water surface. *Q. J. R. Meteorol. Soc.* **1955**, *81*, 639–640. [[CrossRef](#)]
59. Cohen, A.E.; Cavallo, S.M.; Coniglio, M.C.; Brooks, H.E. A review of planetary boundary layer parameterization schemes and their sensitivity in simulating southeastern U.S. cold season severe weather environments. *Weather Forecast.* **2015**, *30*, 591–612. [[CrossRef](#)]
60. Termonia, P.; Fischer, C.; Bazile, E.; Bouyssel, F.; Brožková, R.; Bénard, P.; Bochenek, B.; Degrauwe, D.; Derková, M.; El Khatib, R.; et al. The ALADIN System and its canonical model configurations AROME CY41T1 and ALARO CY40T1. *Geosci. Model Dev.* **2018**, *11*, 257–281. [[CrossRef](#)]
61. Louis, J.F. A parametric model of vertical eddy fluxes in the atmosphere. *Bound. Layer Meteorol.* **1979**, *17*, 187–202. [[CrossRef](#)]
62. Cuxart, J.; Bougeault, P.; Redelsperger, J.L. A turbulence scheme allowing for mesoscale and large-eddy simulations. *Q. J. R. Meteorol. Soc.* **2000**, *126*, 3055–3079. [[CrossRef](#)]
63. Ricard, J.L.; Royer, J.F. A statistical cloud scheme for use in an AGCM. *Ann. Geophys.* **1993**, *11*, 1095–1115.
64. Mellor, G.L.; Yamada, T. A Hierarchy of Turbulence Closure Models for Planetary Boundary Layers. *J. Atmos. Sci.* **1974**, *31*, 1791–1806. [[CrossRef](#)]
65. Bougeault, P.; Lacarrère, P. Parameterization of Orography-Induced Turbulence in a Mesobeta-Scale Model. *Mon. Weather Rev.* **1989**, *117*, 1872–1890. [[CrossRef](#)]
66. Sataloff, R.T.; Johns, M.M.; Kost, K.M. Nonlocal Boundary Layer Vertical Diffusion in a Medium-Range Forecast Model. *Mon. Weather Rev.* **1996**, *124*, 2322–2339.
67. van Meijgaard, E.; von Ulf, L.H.; Lenderink, G.; de Roode, S.R.; Wipfler, L.; Boers, R.; Timmermans, R.M.A. *Refinement and Application of a Regional Atmospheric Model for Climate Scenario Calculations of Western Europe*; Wageningen University: Wageningen, The Netherlands, 2012; pp. 1–46.
68. Holtslag, A.A.M.; Bruijn, E.I.F.d.; Pan, H.L. A High Resolution Air Mass Transformation Model for Short-Range Weather Forecasting. *Mon. Weather Rev.* **1990**, *118*, 1561–1575. [[CrossRef](#)]
69. Bretherton, C.S.; McCaa, J.R.; Grenier, H. A new parameterization for shallow cumulus convection and its application to marine subtropical cloud-topped boundary layers. Part I: Description and 1D results. *Mon. Weather Rev.* **2004**, *132*, 864–882. [[CrossRef](#)]
70. Davies, T.; Cullen, M.J.P.; Malcolm, A.J.; Mawson, M.H.; Staniforth, A.; White, A.A.; Wood, N. A new dynamical core for the Met Office's global and regional modelling of the atmosphere. *Q. J. R. Meteorol. Soc.* **2005**, *131*, 1759–1782. [[CrossRef](#)]
71. Hong, S.Y.; Noh, Y.; Dudhia, J. A new vertical diffusion package with an explicit treatment of entrainment processes. *Mon. Weather Rev.* **2006**, *134*, 2318–2341. [[CrossRef](#)]